THE BEAM LOSS MONITORING SYSTEM IN TAIWAN PHOTON SOURCE

C. H. Huang, Demi Lee, Jenny Chen, Y. S. Cheng, K. H. Hu, C. Y. Wu, P. C. Chiu, K. T. Hsu
NSRRC, Hsinchu 30076, Taiwan

Abstract

Taiwan Photon Source is a third generation and 3 GeV synchrotron light source during beam commissioning in NSRRC. Several types of beam loss monitors (BLMs) such as PIN diodes, scintillation detectors, Cherenkov BLMs and RadFETs are installed in the storage ring and booster ring to study the beam loss distribution and mechanism. The installation infrastructure, design of reader units and integrated graphic user interface will be described in this report. The preliminary experimental results will also be summarized here.

INTRODUCTION

Taiwan Photon Source (TPS) is a third-generation light source in NSRRC [1]. The circumference of the storage ring is 518.4 m with 24 double-bend achromat cells. There are 6 long-straight sections and 18 standard-straight sections to accommodate insertion devices. In the first initial phase for the beam-line commissioning, seven beam lines with ten inserting devices are installed in the storage ring. At the same time, two superconducting RF (SRF) cavities are also installed during this stage.

To study the beam loss during the SRF and inserting device commissioning, several types of beam loss monitors (BLMs) are setup in the storage ring and booster ring. The PIN diodes can detector the minimum ionizing particles as an electron hits the wall of the vacuum chamber and produce the electromagnetic shower [2]. Cherenkov detector is sensitive to charged particles. The scintillation detector is a kind of secondary emission monitor which combines a scintillating material and photomultiplier tube and can detect both the charged particles and X ray. A radiation-sensing field-effect transistor (RadFET) is a metal-oxide-semiconductor field-effect transistor (MOSFET) with an aluminium gate and a thick layer of silicon dioxide which can be used as a dosimeter [3]. These installed BLMs provide a tool to investigate the beam loss location, beam lifetime, vacuum conditions, beam loss mechanism, specific beam loss, resonance crossing, energy measurement by mean of spin depolarization method, etc. These may be also useful to fine tune the machine during the commissioning, routine operation and beam physics study.

PIN-DIODE BEAM LOSS MONITOR

Bergoz's PIN-diode BLM is made of two diodes mounted face-to-face [4]. For the coincidence readout of the signals of two channels, the dual PIN-diode BLM detects charge particles rather than synchrotron radiation and reduces the dart counts due to the noise. It is widely used in many facilities [5]. There are many kinds of solutions to integrate this BLM. To simplify the wiring, a custom designed version of Bergoz's BLM was adopted in which the original 10 pin connector is replaced by a RJ-45 connector as shown in the BLM photo of Fig. 1. The output of the BLM is coupled by a pulse transformer. Four pairs of twisted cables are used to connect a BLM to the signal translator. This twisted cable provides power to a BLM and sends the coincident pulse back. An 8-channel LVDS to LVTTL translator is used to convert pulses. The pulse complied with LVTTL level is connected to the scaler input.

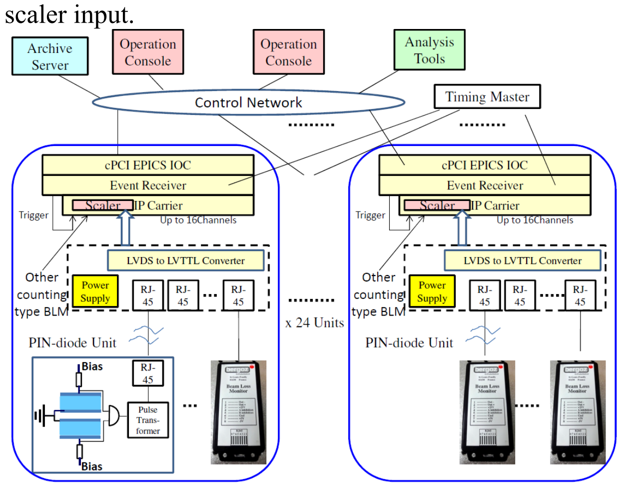

Figure 1: Block diagram of the PIN-diode beam loss monitoring system.

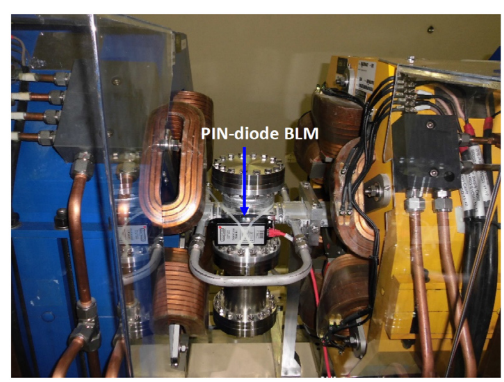

Figure 2: The setup of a PIN-diode BLM.

Data acquisition for BLMs is performed by a 16-channel scaler in an industrial pack (IP) form factor. The IP module is installed on the cPCI carrier board which is located at the cPCI EPICS IOC on the equipment area. All scalers which distributes at 24 IOCs are synchronized by the timing system of the accelerator, shown in Fig. 1. Unused channels of the scalers will be served for another

ISBN 978-3-95450-176-2

kind of counting-type BLMs in the future. Gating period of the scaler is programmable with 1 msec step. The scalar can also operate in the histogram mode with the gate interval in the unit of msec.

Six PIN-diode BLMs in each cell are installed in the inside-wall chamber of the storage ring using cable ties or Kapton tapes as shown in Fig. 2. The setup position of RadFETs for 24 cells is shown Fig. 3. The beam loss distribution in Fig. 4 would be shown with bar chart in the control system.

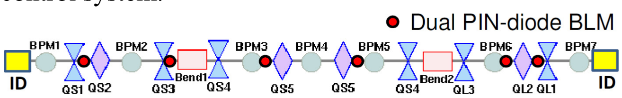

Figure 3: The setup positions of PIN-diode BLMs.

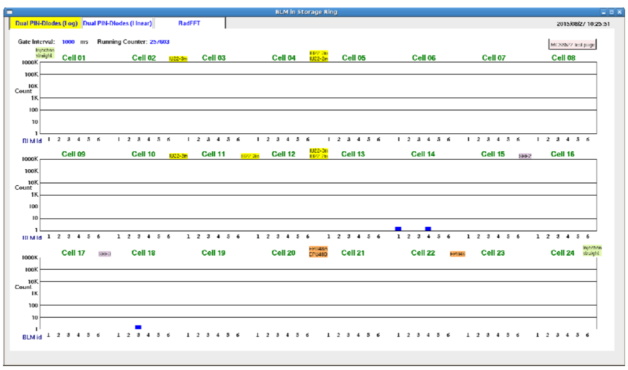

Figure 4: The graphical user interface of PIN-diode BLMs.

RADIATION-SENSING FIELD-EFFECT TRANSISTOR

The RadFET is a discrete p-channel MOSFET optimized for ionizing radiation [6]. The threshold voltage of a RadFET between the gate and source changes due to radiation-induced charges in the oxide layer when applying a constant drain current. The reader of the RadFETs acts as applying constant drain current and reading the threshold periodically. The radiation dose is obtained by a pre-recorded calibration curve between the threshold voltage and radiation dose. The dose rate can be easily obtained by taking time derivative of the recoded dose data.

To obtain high-density installation, the reader is designed up to sixteen channels. A SPI interface is used to read threshold voltage of RadFETs in an ADC. The SPI interface also enables/disables current source in the digital input and output to minimize the interconnecting inside the reader. The process is controlled by the program inside the EPICS IOC, shown in Fig. 5. These sensors can accumulate the radiation dose up to 10K Gray with centigray resolution [7]. Dosage rate is calculated by the EPICS record processing in the EPICS IOC and published into control network.

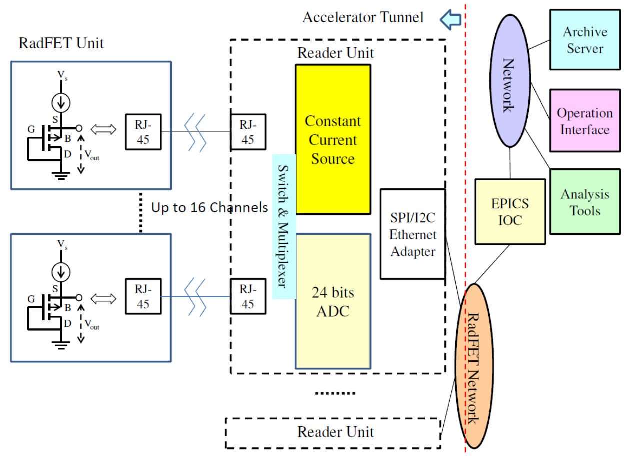

Figure 5: Block diagram of the RadFET setup.

During the Linac and Linac to booster (LTB) commissioning, several RadFETs are installed after the bending magnet, around the dumper and before the stopper. The dose rate updates one minute along accelerator synoptic display, shown in Fig. 6. The threshold voltage of RadFETs are recorded in the archive server, shown in Fig. 7 for further usage. The dose rate or accumulated dose can be processed by a Matlab program from the data in the archive server.

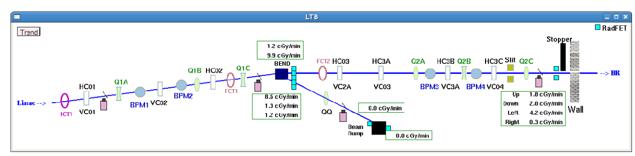

Figure 6: Values along accelerator synoptic display.

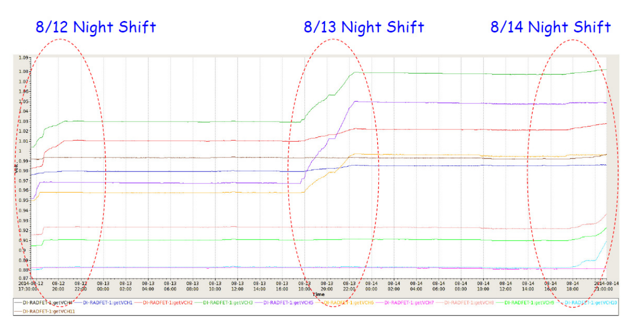

Figure 7: The archived data of the threshold voltages of RadFETs installed in the LTB during the Linac and LTB commissioning form July 12th to 14th, 2014.

RadFETs are also installed before the fifty-four bending magnets of the booster synchrotron in six cells to monitor the beam loss during booster commissioning. Nine RadFETs in each cell are collected by a reader. The threshold voltage, dose, dose rate and beam loss distribution are shown in the control system on line. The beam loss pattern during ramping is shown in Fig. 8.

ISBN 978-3-95450-176-2

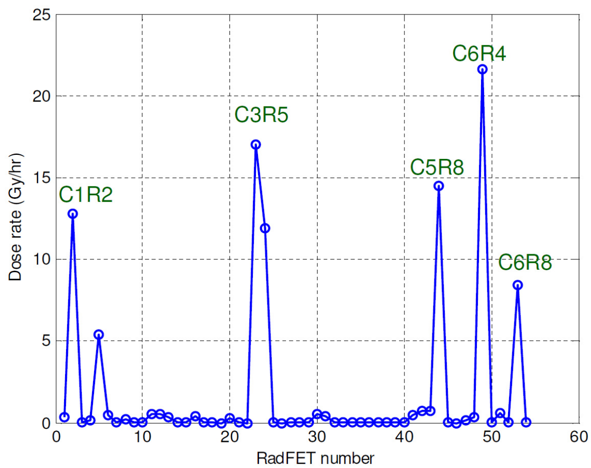

Figure 8: The beam loss pattern as the energy was ramping from 150 MeV to 3 GeV in January 19th, 2015.

In the storage ring, six RadFETs in each cell are installed in the inside wall of the vacuum chamber, shown in Fig. 9(a), in the first stage. These six RadFETs are collected by one reader settled in the cable stray of the tunnel, shown in Fig. 9(b), to minimize the radiation damage and reduce the cable length between the RadFET and reader. Twenty-four readers connect to the EPICS IOC via a private network. The setup position is shown in Fig. 10.

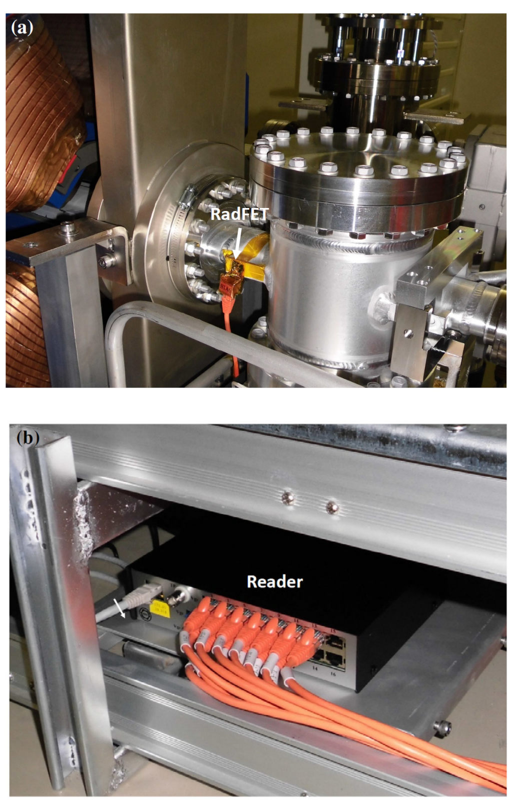

Figure 9: (a) A RadFET and (b) RadFET reader are installed in the inside-wall chamber and cable tray of the storage ring.

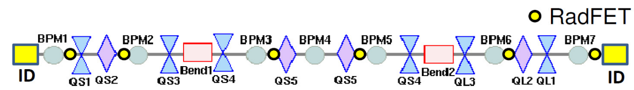

Figure 10: The setup position of RadFETs.

SCINTILLATION-TYPE BEAM LOSS MONITOR

Several high counting rate BLMs are installed in the first cell below the injection straight as shown in Fig. 11. This scintillation detector, in Fig. 12, is consistent of a probe and a photomultiplier tube (PMT) which are connected with a 1m long light pipe [8]. A piece of plastic scintillator which is sensitive to the charge particles is installed in the probe. The diameter of the plastic scintillator is 30 mm and the thickness is 10 mm. The output pulse from the PMT is negative. Another type of signal convert should be designed for the scalar input. In the first stage, the signal is observed by an oscilloscope.

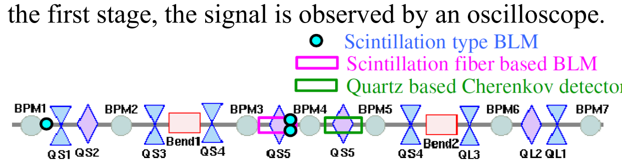

Figure 11: The setup of scintillation and Cherenkov BLMs in the first cell below the injection straight.

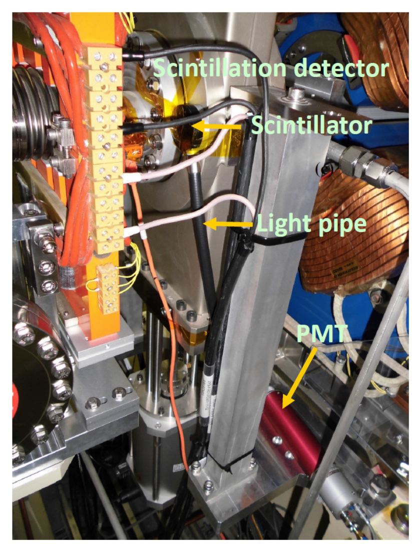

Figure 12: Installation location of a scintillation detector.

MISCELLANEOUS EFFORTS

To equip more beam loss monitors to support various beam loss study, single PIN diode based on solid ionization chamber accompanied with a current to frequency converter is in development. This kind of interface is easy to integrate with the existed scaler. Large volume installation is possible.

Scintillation based BLMs in ESRF type are also considered to be used to support various beam loss study. This detector includes a Zynq based system-on-chip data acquisition unit which supports both the pulse counting

ISBN 978-3-95450-176-2

mode as well as current integration mode. It is above to commercialize soon [9].

A scintillation fiber based BLM which equips with two silicon photomultiplier (SiPM) at both ends is installed in the first cell as shown in Fig. 13. The sensitive volume of the scintillation detector is a plastic scintillating fiber with round cross section of 1 mm diameter. Another quartz rod based Cherenkov-type BLM which equips with two SiPMs at both ends of quartz rode are also installed here to detect the beam loss, shown in Fig. 14. The sensitive volume is a 1.2 cm diameter glass rod with 64 cm sensor length. Signals from both SiPMs can be performed coincident detection to reduce dark counts. These sensors are used to evaluate SiPM type detection at TPS environment. Both kinds of sensors were made by Microsensor S.R.L., Catania, Italy.

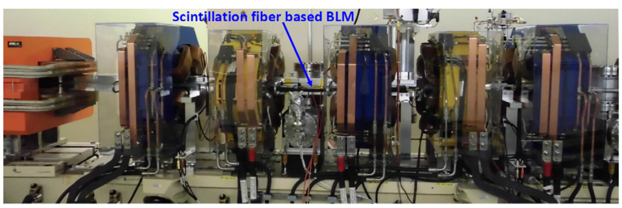

Figure 13: The installation of a scintillation fiber based beam loss monitor.

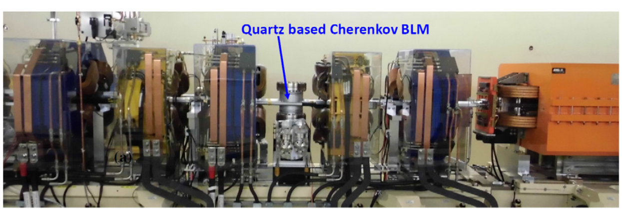

Figure 14: The installation of a quartz based Cherenkov beam loss monitor.

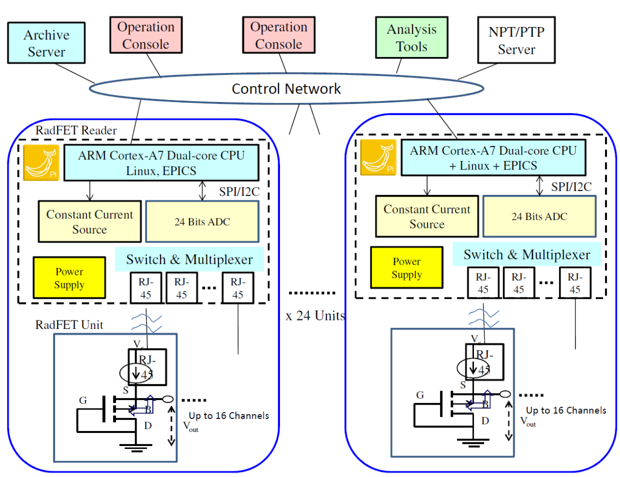

Figure 15: The configuration of the second-generation reader of the RadFET.

Recently, the second-generation reader of the RadFET is in development. The main difference with the first-generation one is that a Banana Pi [10] with ARM Cortex-A7 Dual-core CUP will be embedded inside the reader. Therefore, the Linux, EPICS and controlling program could be installed in the SD card. The configuration is shown in Fig. 15. This reader can also be used stand-alone by recording the data in the SD card as the network is unreachable.

CURRENT STATUS

Phase I commissioning was proceeded with two 5-cell PETRA cavities and without insertion devices from December 2014 to March 2015 [11]. RadFETs are setup in the LTB and booster ring to help beam commissioning. During the long shutdown from April to August, various devices of BLMs are setup in the storage ring. Data acquisition for the counting-type beam loss monitors were setup. The system testing is scheduled in September 2015 which accompanies the phase II commissioning.

ACKNOWLEDGEMENT

Authors thank the brainstorming with Julien Bergoz about how to simplify the cabling of PIN-diode BLMs and conclude a simple twisted-pair solution.

REFERENCE

[1] TPS Design Handbook, version 16, June 2009.
[2] K. Wittenburg, “Beam Loss Monitors”, DESY, Hamburg, Germany.
[3] C. H. Huang et al.,”Beam Loss Study of TLS using RadFETs”, IPAC 2015, Richmond, USA.
[4] Manual of bergoz beam loss monitor, http://www.bergoz.com/
[5] K.T. Hsu et al. “Real-Time Beam Loss Monitoring and its Applications in SRRC”. Particle Accelerator Conference 1997, Vancouver, Canada.
[6] L. Fröhlich, et al., “Online Monitoring of Absorbed Dose in Undulator Magnets with RADFET Dosimeters at FERMI@Elettra”, Nucl. Instr. and Meth. A 703 (2013) 70-79.
[7] Demi Lee et al.,” Online RadFET Reader for Beam Loss Monitoring System”, IPAC 2015, Richmond, USA.
[8] Website of Scionix: http://scionix.nl/.
[9] K. Scheidt and P. Leban, “Prototype Results with a complete Beam Loss Monitor System Optimized for Synchrotron Light Source”, IPAC2015, Richmond, USA.
[10] Website of Banana Pi: http://www.banana-pi.org/ .
[11] C. C. Kuo et al., “Commissioning Results of Taiwan Photon Source”, IPAC 2015, Richmond, USA.

ISBN 978-3-95450-176-2